

Distributionally Robust Statistical Verification with Imprecise Neural Networks

Souradeep Dutta¹, Michele Caprio¹, Vivian Lin¹, Matthew Cleaveland¹, Kuk Jin Jang¹, Ivan Ruchkin², Oleg Sokolsky¹, Insup Lee¹

¹University of Pennsylvania, ²University of Florida
{duttaso, caprio, vilin, mcleav, jangkj, sokolsky, lee}@seas.upenn.edu¹, iruchkin@ece.ufl.edu²

Abstract

A particularly challenging problem in AI safety is providing guarantees on the behavior of high-dimensional autonomous systems. Verification approaches centered around reachability analysis fail to scale, and purely statistical approaches are constrained by the distributional assumptions about the sampling process. Instead, we pose a distributionally robust version of the statistical verification problem for black-box systems, where our performance guarantees hold over a large family of distributions. This paper proposes a novel approach based on a combination of active learning, uncertainty quantification, and neural network verification. A central piece of our approach is an ensemble technique called Imprecise Neural Networks, which provides the uncertainty to guide active learning. The active learning uses an exhaustive neural-network verification tool Sherlock to collect samples. An evaluation on multiple physical simulators in the openAI gym Mujoco environments with reinforcement-learned controllers demonstrates that our approach can provide useful and scalable guarantees for high-dimensional systems.

1 Introduction

A major problem in AI safety is providing guarantees on the behavior of autonomous systems with learning components (Seshia, Sadigh, and Sastry 2022; Divband Soorati et al. 2022). These guarantees can be on safety (“an undesired event will not happen”), liveness (“a desired event will eventually happen”), average performance (“the mean outcome is acceptable”), or generalized rewards (Song et al. 2022; Mitra 2021; Cubuktepe et al. 2020). A typical role of learning components is to perceive a complex environment or make decisions about how to control the system — the latter are often trained with reinforcement learning. It is increasingly common to combine perception and control into a deep neural architecture (e.g., “pixel-to-action control” (Michelmore et al. 2020; Tomar et al. 2022)).

While model-based formal verification can give exhaustive guarantees on low-dimensional systems, high-dimensional ones are practically analyzed with black-box statistical approaches (Corso et al. 2022; Zarei, Wang, and Pajic 2020; Lew et al. 2022; Moss et al. 2023; Qin et al. 2021). Such approaches as confidence intervals (Park et al.

2021), hypothesis testing (Farid, Veer, and Majumdar 2022), and conformal inference (Lindemann et al. 2023) derive confidence-based guarantees from a finite sample of trajectories. Active learning with Gaussian Processes (GPs) can make sampling more efficient by guiding it toward higher-uncertainty regions of initial states (e.g., the location where an autonomous car starts a scenario) and dynamics parameters (e.g., the maximum braking power).

Existing approaches to statistical verification give guarantees with respect to a *single, fixed distribution* of initial states or system parameters (often implicitly so) (Qin et al. 2021). In real-world deployments, it is difficult to predict or impose an exact distribution of states/parameters. As a result, the up-front statistical guarantees may be disrupted by the distribution shift of real-world deployments (Sinha et al. 2022). Furthermore, when it comes to realistic autonomous systems with higher (10+) dimensions, uncertainty quantification with GPs has limited scalability and sample efficiency (Liu et al. 2020).

This paper proposes an approach to distributionally robust statistical verification with active learning. Instead of assuming a fixed distribution of initial states, we pose the problem of finding a *family of distributions* that can uphold an expected lower bound on the desired performance metric given a specified level of confidence. The resulting family describes a variety of deployment scenarios where our performance guarantee applies and, therefore, can be used as part of pre-deployment validation and online monitoring.

At the heart of our approach is a surrogate performance model of a black-box autonomous system implemented with a novel ensemble technique called *Imprecise Neural Network* (INN) (Oala et al. 2020; Caprio et al. 2022). The uncertainty measure provided by the INN guides the sampling process, which alternates with scalable re-training of the INN. We pair the INN with a neural-network verification tool SHERLOCK (Dutta, Chen, and Sankaranarayanan 2019; Dutta et al. 2018a) to obtain distributional guarantees within a neighborhood of the sampled points.

We evaluate our approach on 10 case studies of physics simulators (Mujoco, OpenAI Gym (Brockman et al. 2016)) with neural-network perception and control. The experiments show that our family-wide guarantees indeed apply in practice, our uncertainty quantification scales well to higher dimensions, and our approach is more robust to distribution

arXiv:2308.14815v2 [cs.AI] 30 Aug 2023

shift than the baseline of conformal prediction.

Thus, this paper makes four contributions:

- A novel formulation of distributionally robust statistical verification that enables a combination of statistical and exhaustive guarantees.
- A scalable active learning algorithm that combines imprecise neural networks with formal verification.
- A theoretical guarantee on the system’s worst-case performance for any distribution in a produced family. This allows us to extend our guarantees outside of the training distribution.
- An experimental evaluation on a variety of autonomy benchmarks from OpenAI gymnasium.

2 Problem and Approach

Problem Formulation

Consider an autonomous system $x_{t+1} \sim F(x_t)$, where $x \in \mathbb{R}^n$ and F is a stochastic vector-valued function that dictates the evolution of the system over time. In practice, F captures the composition of system dynamics with the control policy, and x belongs to a closed and compact set \mathcal{X} . Starting from some initial state x_0 , and executing the closed-loop system for T steps generates a trajectory $\tau_{x_0} := [x_0, x_1, \dots, x_T]$, such that $x_{i+1} \sim F(x_i)$. Additionally, the real-valued random *performance variable* ψ assigns a scalar to the trajectory τ_{x_0} , and is thus dependent on x_0 . It quantifies the performance or the degree of satisfaction of a desired property by trajectory τ_{x_0} . Our goal is to obtain some performance guarantees when the initial value x_0 is drawn from set $\mathcal{X}_0 \subseteq \mathcal{X}$. The set \mathcal{X}_0 can be part of a high-dimensional space, rendering it computationally prohibitive to sample densely. Now, we expect x_0 to be drawn according to some to-be-discovered set of distributions over this initial set \mathcal{X}_0 . Our goal will be to lower-bound the chance of performance function ψ exceeding some threshold ϵ for any distribution in the above set. We instantiate this problem more concretely below:

Problem: Consider a set of initial states \mathcal{X}_0 , a performance function ψ , and a confidence parameter $\lambda > 0$. Let $A = \{\psi(x_0) \geq \epsilon\}$, for some performance threshold $\epsilon > 0$. We want to find an ϵ and a family of distributions \mathcal{P} over the space $\mathcal{X}_0 \times \mathbb{R}$ of initial states and performances, such that — in expectation — the conditional probability of event A when sampling initial states x_0 from any distribution in $\mathcal{P}_{\mathcal{X}_0}$ is at least $(1 - \frac{1}{\lambda})$. Here, $\mathcal{P}_{\mathcal{X}_0}$ is the set of marginals of the elements of \mathcal{P} over \mathcal{X}_0 . Mathematically, this means that

$$\mathbb{E}_{X \sim P_{\mathcal{X}_0}} [P_{\psi(x_0)|X=x_0}(\psi(x_0) \geq \epsilon)] \geq \left(1 - \frac{1}{\lambda}\right) \quad (1)$$

for all $P_{\mathcal{X}_0} \in \mathcal{P}_{\mathcal{X}_0}$ and all conditional probabilities $P_{\psi(x_0)|X=x_0}$.

To elaborate further, the term $P_{\psi(x_0)|X=x_0}(\psi(x_0) \geq \epsilon)$ captures the probability that the system’s performance is above some threshold ϵ , under the stochasticity of the system’s evolution function F . Moreover, an additional challenge lies in the fact we want this to hold over a family of

distributions $\mathcal{P}_{\mathcal{X}_0}$. The expectation computes the fraction of samples expected to satisfy event A when the x_0 ’s are drawn from the distribution $P_{\mathcal{X}_0}$. The inequality above demands that this expectation is above a threshold of $(1 - \frac{1}{\lambda})$.

Overall Approach

Performance guarantees in high dimensional spaces are computationally hard due to the inherent dependency on the sampling process. This necessitates an efficient uncertainty-guided sampling process, similar to Gaussian process regression but more scalable. To this end, we propose an efficient exploration strategy, followed by an exhaustive search that computes a lower performance bound. The above steps will rely on the neural-network verification tool SHERLOCK (Dutta et al. 2019, 2018b). We use the following two-step process to estimate the lower bound outlined in the problem statement above.

1. **Active Learning Strategy:** This step learns an *Imprecise Neural Network (INN)* $\{\underline{\Phi}(x), \bar{\Phi}(x)\}$, which estimates the bounds on $\psi(x_0)$ by drawing from samples x_0 from \mathcal{X}_0 . Explained in Section 4, INNs enable a novel notion of *network uncertainty* computed as the width $w := [\bar{\Phi} - \underline{\Phi}](x)$, and we show that it satisfies the basic mathematical requirements of being an uncertainty measure. To implement efficient sampling in high dimensions, we propose an active learning strategy where SHERLOCK computes regions of high uncertainty in \mathcal{X}_0 as measured by the width w . Our active learning proceeds in a greedy fashion by sampling points from high-uncertainty regions and using ψ to estimate the ground-truth performance. This sample-efficient active-learning process is terminated after a finite number of steps. The explored regions help us in constructing the set of distributions over which the guarantees in Eq. 1 hold.

2. **Computing Performance Limits:** The INN $\{\underline{\Phi}(x), \bar{\Phi}(x)\}$ captures the upper and lower estimates of the performance function over a certain subset $\mathcal{X}' \subseteq \mathcal{X}_0$ of the initial set \mathcal{X}_0 . This subset \mathcal{X}' results from the exploration in the previous step. We aim to find a worst-case bound on the lower estimate of the INN over \mathcal{X}' , that is $\Phi^l = \min_{x \in \mathcal{X}'} \underline{\Phi}(x)$. We rely on SHERLOCK

to compute Φ^l , serves as the lower bound over a set of distributions \mathcal{P} . We explain in Section 4 how to construct the set of probability distributions \mathcal{P} such that, $\mathbb{E}_{X \sim P_{\mathcal{X}_0}} [P_{\psi(x_0)|X=x_0}(\psi(x_0) \geq \epsilon)] \geq (1 - \frac{1}{\lambda})$, $\forall P_{\mathcal{X}_0} \in \mathcal{P}_{\mathcal{X}_0}$ and all conditional probabilities $P_{\psi(x_0)|X=x_0}$ by setting $\epsilon = \Phi^l$.

3 Related Work

Statistical guarantees for autonomy Traditional approaches to statistical assurance are based on confidence intervals (Gupta, Podkopaev, and Ramdas 2022; Alasmari et al. 2022) and hypothesis tests (Farid, Veer, and Majumdar 2022; Wang et al. 2021; Larsen and Legay 2014). Recently though, due to its distribution-free nature, conformal prediction (CP) has become particularly popular (Luo et al. 2023; Cleaveland et al. 2022; Cairoli, Bortolussi, and Paoletti

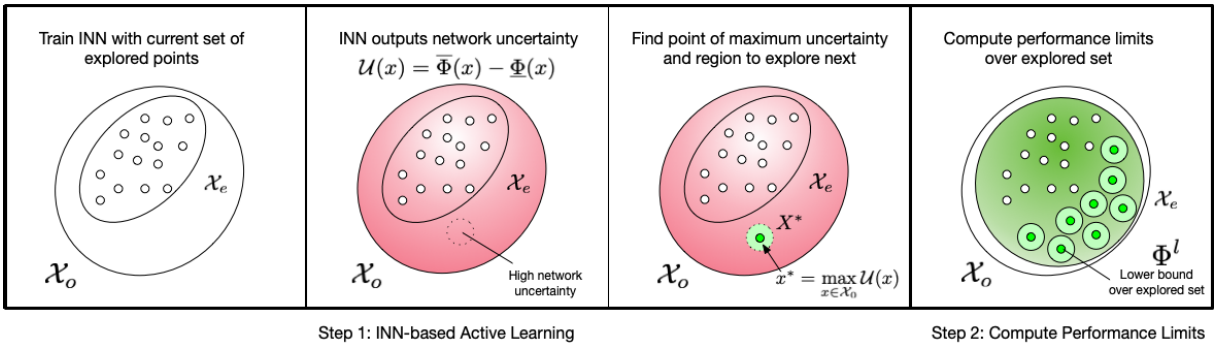


Figure 1: Here \mathcal{X}_0 is explored across several iterations by employing an active learning strategy based on Imprecise Neural Networks (INN). At each iteration, given the current set of explored points $\mathcal{X}_e \in \mathcal{X}_0$, an INN model is trained, which outputs the network uncertainty $\mathcal{U}(x)$ over \mathcal{X}_0 . Using Sherlock (Dutta et al. 2018a), a sample which maximizes the uncertainty, x^* , is obtained. Next, a local δ -ball region, X^* , is sampled uniformly to be explored. The INN model is updated by including the newly explored samples. Finally, at the end of all iterations INN model (after M iterations) and \mathcal{X}_e are used to compute the lower bound of performance Φ^l .

2021; Qin et al. 2021; Muthali et al. 2023). In short, it makes a statistical guarantee on the non-conformity score of the next sample given a calibration set (Vovk, Gammernan, and Shafer 2005; Shafer and Vovk 2008) — as long as the sample and the set are drawn exchangeably from some unknown distribution (without any assumptions on its shape or family). However, conformal prediction does not provide guarantees with respect to sets of distributions, so it has a limited ability to handle a distribution shift. Our experiments in Sec. 6 investigate the differences between the single-distribution CP setting and our robust formulation. Another recent work leverages random set theory to improve the sample efficiency and error bounds of sampling-based reachability (Lew et al. 2022), which would be interesting to combine with imprecise neural networks. An adjacent area is the testing and falsification of neural networks, which can be understood as an (often sampling-based) exploration of the network’s input-output relation (Du et al. 2022; Chakraborty and Bansal 2023; Zhang et al. 2023; Dreossi et al. 2019), but aimed to satisfy the testing criteria (e.g., coverage) rather than establish performance guarantees.

Uncertainty quantification and active learning The goal of uncertainty quantification (Smith 2013; Sullivan 2015) is to compute a measure of trust towards a model’s output, with typical methods including Bayesian neural networks (Michelmoro et al. 2020; Cardelli et al. 2019; Wicker et al. 2020), ensembles (Seung, Opper, and Sompolinsky 1992; Lakshminarayanan, Pritzel, and Blundell 2017; Pearce et al. 2018), and confidence calibration (Guo et al. 2017; Minderer et al. 2021). Gaussian processes (GPs) (Rasmussen and Williams 2005) are a popular tool for data-driven modeling and uncertainty quantification in autonomy (Aoude et al. 2013; Bansal et al. 2018; Castaneda et al. 2021). Specifically, it is frequently used in the state-of-the-art statistical verification methods to guide the sampling based on the Gaussian uncertainty (Qin et al. 2021; Moss et al. 2023; Petrov et al. 2022). Due to the challenges with scalability (Liu et al. 2020), GPs fall short as an uncertainty quantifier in high-dimensional black-box systems — as demonstrated in our experiments.

Imprecision in Neural Networks To effectively verify input-output properties on neural networks, set-based computation is typically implemented via overapproximation and abstractions (Dutta et al. 2018a; Sidrane et al. 2022; Gehr et al. 2018; Ashok et al. 2020; Ladner and Althoff 2023). However, this setting is usually non-stochastic. To gauge uncertainty in the regression analysis at hand, several techniques based on the imprecise probabilities literature (Troffaes and de Cooman 2014; Walley 1991) have been developed. The most recent ones are Imprecise Bayesian Neural Networks (IBNNs) (Caprio et al. 2022), that give a principled way of carrying out a regression via credal sets, and Evidential Neural Networks (ENNs) (Denoeux 2022), that instead use fuzzy logic. In (Tretiak, Schollmeyer, and Ferson 2022), the authors present an Imprecise Probability based neural network which uses a regression technique based on probability intervals. Contrary to IBNNs and ENNs, their neural network is rooted in the frequentist approach to imprecise probabilities (Huber and Ronchetti 2009).

4 Methodology

Preliminaries

In this section we detail the working of the proposed algorithm. To reiterate our goal, given an oracle function $\psi : \mathcal{X} \rightarrow \mathbb{R}$, we wish to compute a family of joint distributions \mathcal{P} and a lower bound ϵ such that for any marginal distribution $P_{\mathcal{X}_0}$ in $\mathcal{P}_{\mathcal{X}_0}$, the expectation that $\psi(x_0) \geq \epsilon$, for $x_0 \sim P_{\mathcal{X}_0}$ is lower bounded by $(1 - \frac{1}{\lambda})$. Since, ψ is a black-box function, we use a regression based technique which estimates the function ψ . The model for our regression here is an Imprecise Neural Network (INN) which builds on standard DNNs. This is defined as the following,

Definition 1 (Imprecise Neural Network). Given a set of deep neural networks $\{f_1, f_2, \dots, f_k\}$ where $f_i : \mathcal{X} \rightarrow \mathcal{Y}$, an Imprecise Neural Network is given by a tuple $\{\underline{\Phi}(x), \bar{\Phi}(x)\}$, where $\bar{\Phi}(x) = \max_{i \in [k]} f_i(x)$ and $\underline{\Phi}(x) = \min_{i \in [k]} f_i(x)$.

In our case \mathcal{Y} is the set of reals \mathbb{R} . However, in a multi-dimensional case the *max/min* is taken element wise. The intention behind using INNs is that instead of computing the

exact estimate of the ground-truth value, we wish to compute upper and lower bound estimates of the ground truth. This can be accomplished using a carefully crafted loss function shown in Equation 3. A salient feature that one derives from this is a novel way to quantify uncertainty, which is defined as follows:

Definition 2 (Network Uncertainty). Given an Imprecise Neural Network $\{\underline{\Phi}(x), \overline{\Phi}(x)\}$, the uncertainty at $x \in \mathcal{X}$ is defined as $\mathcal{U}(x) = \overline{\Phi}(x) - \underline{\Phi}(x)$.

Hence, larger the *disagreement* among the constituent networks which form the INN, the higher the uncertainty. This measure should be intuitive since, for parts of the space where no data was observed, randomly initialized DNNs are more likely to disagree. We further justify the choice of using this width as a measure of uncertainty in Section 5.

Optimization over DNN Next, we consider the problem of optimizing the inputs to a deep neural network with an objective to maximize/minimize the output. Exact solutions of this problem are generally hard due to its NP-complete nature (Katz et al. 2017). However, due to the big ramifications of solving this problem in the context of verifying of neural networks, this has received much attention (Elboher, Gottschlich, and Katz 2019; Fazlyab, Morari, and Pappas 2019; Dutta, Chen, and Sankaranarayanan 2019; Tran et al. 2020; Ivanov et al. 2021). In this paper, we use one such neural network verification tool SHERLOCK (Dutta et al. 2019) which uses a mixed integer linear program (MILP) encoding of a DNN, with gradient guided search to solve this optimization problem. At a high-level for $x \in$ convex set S , and f_i a DNN, SHERLOCK can compute an interval $[m, M]$, where $m = \min_{x \in S} f_i(x)$ and $M = \max_{x \in S} f_i(x)$. Extension of this search to an INN is straightforward. This is because the output of an INN simply chooses the maxima/minima over a finite number $[k]$ of constituent DNNs.

Algorithms

In general, estimating the nature of ψ by sampling densely over a space of higher dimensions (> 10) is computationally intractable. This means that virtually any algorithm would gain from an efficient sampling schema. In the literature, sample efficiency is often achieved using *forward*-looking techniques which first sample and then examine uncertainty estimates. An example of this is using Gaussian processes, wherein uncertainty estimates on predictions are given for a sample input after evaluation. However, what we find useful here is a *backward* looking technique, where the learner could come up with query points $x_0 \in \mathcal{X}_0$ on account of its own intrinsic curiosity.

This paradigm is similar to Active Learning (AL) (Burbidge, Rowland, and King 2007) in the literature. In AL the learner has access to an oracle function, which can be used to query for ground truth labels instead of a labelled training dataset. Due to the expensive nature of this query, it is in the best interest of the learner to minimize the number of such queries. However a common assumption in the standard active-learning setting is that the learner has access to a finite set of unlabelled input samples. In our setting

Algorithm 1: Active Learning

Input: Oracle function ψ , set \mathcal{X}_0 ,
Output: An INN $\{\underline{\Phi}(x), \overline{\Phi}(x)\}$, explored set \mathcal{X}_e
Parameters: Iteration Count : M , Neighborhood Size : δ

- 1: $\mathcal{T} := \{(x_i, y_i)\}_{i=1}^N \leftarrow$ Draw samples from \mathcal{X}_0 , and assign labels using ψ
 {These samples can be picked according to some desirable starting distribution as well. }
- 2: $\{\underline{\Phi}(x), \overline{\Phi}(x)\} \leftarrow$ Train INN on \mathcal{T} using Equation 3
- 3: $\mathcal{X}_e = \mathcal{X}_0$
- 4: **for** $k = 1$ to M **do**
- 5: $x^* \leftarrow$ Maximize Uncertainty \mathcal{U} in INN
- 6: $\mathcal{T}^* := \{(x_i, y_i)\}_{i=1}^N \leftarrow$ Draw samples uniformly from set $\mathcal{X}^* = \{x : \|x - x^*\|_\infty \leq \delta\}$, and assign labels using ψ
- 7: $\mathcal{X}_e = \mathcal{X}_e \cup \mathcal{X}^*$ and $\mathcal{T} = \mathcal{T} \cup \mathcal{T}^*$
- 8: $\{\underline{\Phi}(x), \overline{\Phi}(x)\} \leftarrow$ Retrain INN on \mathcal{T} using loss in Equation 3
- 9: **end for**
- 10: **return** $\{\underline{\Phi}(x), \overline{\Phi}(x)\}, \mathcal{X}_e$

Algorithm 2: Computing Performance Limits

Input: An INN $\{\underline{\Phi}(x), \overline{\Phi}(x)\}$, explored set \mathcal{X}_e
Output: Lower bound Φ^l

- 1: $C = \phi$
- 2: **for** subset $\mathcal{X}' \subseteq \mathcal{X}_e$ **do**
- 3: local-minima \leftarrow Compute minima of INN $\{\underline{\Phi}(x), \overline{\Phi}(x)\}$ in set \mathcal{X}'
- 4: $C = C \cup$ local-minima
- 5: **end for**
- 6: INN-Minima = Compute lowest value in C
- 7: **return** INN-Minima - $\lambda\beta$

however this does not hold. As stated before, we are aware of some real valued compact set \mathcal{X}_0 , where the input samples are drawn from, and the learner proposes new points to sample. This is captured in the *active learning algorithm* (Algorithm 1). Depending on the uncertainty expressed by the INN, the learner chooses to sample different regions of the input space.

Algorithm for Active Learning As outlined in Algorithm 1, the INN $\{\underline{\Phi}(x), \overline{\Phi}(x)\}$ is randomly initialized with some starting distribution and trained using the correct loss function outlined in Equation 3. Next, at each iteration in the loop (Lines 4 – 9), we use SHERLOCK to maximize uncertainty $\mathcal{U}(x) = \overline{\Phi}(x) - \underline{\Phi}(x)$ in the INN’s predictions. This returns a point x^* which we use to obtain further samples. We draw samples uniformly from a δ -ball (\mathcal{X}^*) centered at x^* , and obtain its labels using an oracle function ψ . Next, (Lines 7 – 8) we add these samples to our current collection of training samples and retrain the INN. Note, that at the end of the active-learning iterations we simply return the explored region \mathcal{X}_e as a union of intervals in the space \mathcal{X} . We maintain this representation of \mathcal{X}_e for ease of implementation of the subsequent algorithms. It is not hard to see that our training distribution is a mixture of uniform distributions defined over these intervals.

Algorithm for Computing Performance Limits The aim of Algorithm 2 is to find the lowest estimate $\underline{\Phi}(x)$ assigned by the INN. This again is an NP-complete problem and can be computationally challenging. However, we can use SHERLOCK to compute this minima for different regions explored in the sampling process when building the set \mathcal{X}_e . This is captured in Line 3, where the local minima is computed by solving $\min_{x \in \mathcal{X}'} \underline{\Phi}(x)$, for a subset \mathcal{X}' in \mathcal{X}_e .

We perform this repeatedly in the loop (Lines 2 – 5), and compute the *INN-minima* over all such values (Line 6). We return this INN-minima after subtracting the $\lambda\beta$ term, as outlined in Theorem 3.

Constructing the family of distributions We define the family of distributions over \mathcal{X} in our analysis as follows. Note, that due to the nature of Algorithm 1, the explored set can be expressed as a union over finite number of subsets, $\mathcal{X}_e = \mathcal{X}_1 \cup \dots \cup \mathcal{X}_m$. Let u_j denote the pdf of the uniform distribution over \mathcal{X}_j , for all $j \in \{1, \dots, m\}$. Then, consider probability measure \tilde{P} whose pdf \tilde{p} is given by a (convex) mixture of the uniforms. That is, $\tilde{p}(x) = \sum_{j=1}^m \gamma_j u_j(x)$, for all $x \in \mathcal{X}$, and a collection of coefficients $\{\gamma_j\}$ whose elements are nonnegative and sum up to 1. Our family is defined as $\mathcal{P}_{\mathcal{X}} := \{P_X : P_X = (1-\delta)\tilde{P} + \alpha Q, \text{ where } Q \text{ is any distribution on } \mathcal{X}\}$, for some $\alpha \in (0, 1)$. This is called a *α -contaminated class* (Caprio et al. 2023; Huber and Ronchetti 2009). Notice that, as a result, the uniform over the whole \mathcal{X} is included in $\mathcal{P}_{\mathcal{X}}$. We have that the upper probability \overline{P}_X – formally introduced in the next section – is given by $\overline{P}_X = (1 - \alpha)\tilde{P} + \alpha$ (Wasserman and Kadane 1990, Example 3).

5 Theory

Recall that a *credal set* is a convex set of probabilities. It is called a *finitely generated credal set* if it has finitely many extreme elements.¹ For a given set \mathcal{P} of probabilities on a generic measurable space (Ω, \mathcal{F}) , its *upper probability* is defined as the upper envelope, that is, $\overline{P}(A) := \sup_{P \in \mathcal{P}} P(A)$, for all $A \in \mathcal{F}$. Similarly, the *lower probability* is the lower envelope, that is, $\underline{P}(A) := \inf_{P \in \mathcal{P}} P(A)$, for all $A \in \mathcal{F}$. In addition, upper and lower probabilities are conjugate to each other, i.e. $\overline{P}(A) = 1 - \underline{P}(A^c)$, for all $A \in \mathcal{F}$.

Call $(\mathcal{X}, \mathcal{A}_{\mathcal{X}})$ the measurable space of inputs and $(\mathcal{Y}, \mathcal{A}_{\mathcal{Y}})$ the measurable space of outputs. Consider a set of probability measures \mathcal{P} on $(\mathcal{X} \times \mathcal{Y}, \mathcal{A}_{\mathcal{X} \times \mathcal{Y}})$. Suppose that every element P in \mathcal{P} can be decomposed as $P(X, Y) = P(X)P(Y | X) \equiv P_X(X)P_{Y|X}(Y)$. This entails that \mathcal{P} can be decomposed in $\mathcal{P}_{\mathcal{X}}$ and $\mathcal{P}_{\mathcal{Y}|\mathcal{X}}$, that is, for every $P \in \mathcal{P}$, we can find $P_X \in \mathcal{P}_{\mathcal{X}}$ and $P_{Y|X} \in \mathcal{P}_{\mathcal{Y}|\mathcal{X}}$ such that $P(X, Y) = P_X(X)P_{Y|X}(Y)$. In turn, this implies that we can write the lower probability \underline{P} associated with \mathcal{P} as the product of the lower probability \underline{P}_X associated with $\mathcal{P}_{\mathcal{X}}$ and the lower probability $\underline{P}_{Y|X}$ associated with $\mathcal{P}_{\mathcal{Y}|\mathcal{X}}$. Similarly, this is true for upper probability \overline{P} . Notice that we

¹The extreme elements are the ones that cannot be written as a convex combination of one another.

implicitly consider geometric conditioning (Gong and Meng 2021), that is,

$$\underline{P}_{Y|X}(Y) = \frac{P(X, Y)}{\underline{P}_X(X)}, \quad (2)$$

and similarly for upper probabilities. We assume that the true joint distribution is in \mathcal{P} , the true marginal for X is in $\mathcal{P}_{\mathcal{X}}$ and the true conditional is in $\mathcal{P}_{\mathcal{Y}|\mathcal{X}}$.

Now consider the following loss function which is an imprecise version of (Oala et al. 2020, Equation (2)),

$$\begin{aligned} \mathcal{L}(\underline{\Phi}, \overline{\Phi}) := & \sup_{P_X \in \mathcal{P}_{\mathcal{X}}} \int_{\mathcal{X}} \left[\sup_{P_{Y|X} \in \mathcal{P}_{\mathcal{Y}|\mathcal{X}}} \int_{\mathcal{Y}} \max(y - \overline{\Phi}(x), 0)^2 P_{Y|X}(dy) \right. \\ & + \sup_{P_{Y|X} \in \mathcal{P}_{\mathcal{Y}|\mathcal{X}}} \int_{\mathcal{Y}} \max(\underline{\Phi}(x) - y, 0)^2 P_{Y|X}(dy) \\ & \left. + \beta (\overline{\Phi}(x) - \underline{\Phi}(x)) \right] P_X(dx), \end{aligned} \quad (3)$$

where $\beta > 0$ is the tightness parameter. Using a loss function that comprises credal sets allows to account for the worst case scenario, and so to obtain a more conservative but more robust outcome. To ease notation, (3) can be rewritten as

$$\mathcal{L}(\underline{\Phi}, \overline{\Phi}) := \overline{\mathbb{E}}_X [\overline{\mathbb{E}}_{Y|X}(\overline{m}^2) + \underline{\mathbb{E}}_{Y|X}(\underline{m}^2) + \beta (\overline{\Phi}(x) - \underline{\Phi}(x))],$$

where

- $\overline{m} := \max(y - \overline{\Phi}(x), 0)$,
- $\underline{m} := \max(\underline{\Phi}(x) - y, 0)$,
- $\overline{\mathbb{E}}_{Y|X}(\overline{m}^2) := \int_{\mathcal{Y}} \max(y - \overline{\Phi}(x), 0)^2 P_{Y|X}(dy)$
- $\underline{\mathbb{E}}_{Y|X}(\underline{m}^2) := \int_{\mathcal{Y}} \max(\underline{\Phi}(x) - y, 0)^2 P_{Y|X}(dy)$,
- for a generic functional g on \mathcal{Y} , $\overline{\mathbb{E}}_{Y|X}(g) := \sup_{P_{Y|X} \in \mathcal{P}_{\mathcal{Y}|\mathcal{X}}} \int_{\mathcal{Y}} g(y) P_{Y|X}(dy)$,
- for a generic functional f on \mathcal{X} , $\overline{\mathbb{E}}_X(f) := \sup_{P_X \in \mathcal{P}_{\mathcal{X}}} \int_{\mathcal{X}} f(x) P_X(dx)$.

The following is our main result on an INN $\{\underline{\Phi}(x), \overline{\Phi}(x)\}$

Theorem 3. Pick any $\lambda > 0$ and any pair (x, y) sampled from a distribution in \mathcal{P} . Let $A = \{\underline{\Phi}(x) - \lambda\beta \leq y \leq \overline{\Phi}(x) + \lambda\beta\}$. If $\mathcal{P}_{\mathcal{X}}$ and $\mathcal{P}_{\mathcal{Y}|\mathcal{X}}$ are compact, then²

$$\begin{aligned} \overline{\mathbb{E}}_X [\underline{P}_{Y|X}(A)] = & \inf_{P_X \in \mathcal{P}_{\mathcal{X}}} \int_{\mathcal{X}} \underline{P}_{Y|X}(\{\underline{\Phi}(x) - \lambda\beta \leq y \leq \overline{\Phi}(x) + \lambda\beta\}) P_X(dx) \\ & \geq 1 - \frac{1}{\lambda}. \end{aligned}$$

²Here and in the rest of the paper, compact has to be understood with respect to the topologies $\sigma(\text{ba}(\mathcal{A}_{\mathcal{X}}); B(\mathcal{A}_{\mathcal{X}}))$ and $\sigma(\text{ba}(\mathcal{A}_{\mathcal{Y}}); B(\mathcal{A}_{\mathcal{Y}}))$, respectively. Recall that $\text{ba}(\Sigma)$ is the set of all bounded finitely additive (signed) measures on a generic sigma-algebra Σ , and $B(\Sigma)$ is the set of all bounded and Σ -measurable functions.

We have two corollaries.

Corollary 4. Pick any $\lambda > 0$ and any pair (x, y) sampled from a distribution in \mathcal{P} . Let $A = \{\underline{\Phi}(x) - \lambda\beta \leq y \leq \overline{\Phi}(x) + \lambda\beta\}$. If $\mathcal{P}_{\mathcal{X}}$ and $\mathcal{P}_{\mathcal{Y}|\mathcal{X}}$ are compact, then

$$\mathbb{E}_X [\overline{P}_{Y|X}(A)] - \mathbb{E}_X [P_{Y|X}(A)] \leq \frac{1}{\lambda}.$$

Corollary 5. Pick any $\lambda, \alpha > 0$ and any pair (x, y) sampled from a distribution in \mathcal{P} . If $\mathcal{P}_{\mathcal{X}}$ and $\mathcal{P}_{\mathcal{Y}|\mathcal{X}}$ are compact, then

$$\begin{aligned} \mathbb{E}_X [\mathbf{1} \{ \overline{P}_{Y|X}(y < \underline{\Phi}(x) - \lambda\beta, y > \overline{\Phi}(x) + \lambda\beta) > \alpha \}] \\ \leq \frac{1}{\lambda\alpha}, \end{aligned}$$

where $\mathbf{1}\{\cdot\}$ denotes the indicator function.

From an applied point of view, the requirements of $\mathcal{P}_{\mathcal{X}}$ and $\mathcal{P}_{\mathcal{Y}|\mathcal{X}}$ being compact are easy to satisfy. For instance, it is enough for them to be finite sets or finitely generated credal sets.

INN Uncertainty

In this work, we are interested in the input elements $x \in \mathcal{X}$ whose *network uncertainty* is high. The latter is defined as $\mathcal{U}(x) = \overline{\Phi}(x) - \underline{\Phi}(x)$. After training, we use SHERLOCK to sample elements from regions of the input space \mathcal{X} where the network uncertainty is maximal. By doing this, our aim is that of exploring the regions of \mathcal{X} that we do not observe during training. We call this endeavor *input space curiosity*.

Let us note in passing that network uncertainty is a good measure of uncertainty both from an intuitive and a mathematical viewpoint. Intuitively, we have the highest $\mathcal{U}(x)$ for the elements $x \in \mathcal{X}$ that the neural networks disagree about the most. This conveys the idea of (high) uncertainty. Mathematically, we have that

- (1) $0 \leq \mathcal{U}(x) < \infty$, for all $x \in \mathcal{X}$;
- (2) $\mathcal{U}(x)$ corresponds to the Lebesgue measure of the segment $[\underline{\Phi}(x), \overline{\Phi}(x)]$, and is therefore a continuous functional.
- (3) $\mathcal{U}(x)$ is monotone. To see this, let $x, x' \in \mathcal{X}$ and suppose that $\underline{\Phi}(x') \leq \underline{\Phi}(x)$ and $\overline{\Phi}(x') \geq \overline{\Phi}(x)$. Then, $[\underline{\Phi}(x), \overline{\Phi}(x)] \subseteq [\underline{\Phi}(x'), \overline{\Phi}(x')]$ and $\mathcal{U}(x) \leq \mathcal{U}(x')$.
- (4) $\mathcal{U}(x)$ exhibits probability consistency. That is, if $\underline{\Phi}(x) = \overline{\Phi}(x)$, then $\mathcal{U}(x) = 0$.

As pointed out by (Abellán and Klir 2005; Jiroušek and Shenoy 2018), a suitable measure of credal uncertainty should satisfy properties (1)-(4). Although interval $[\underline{\Phi}(x), \overline{\Phi}(x)]$ is not a credal set, it is heuristically similar to an interval of measure (IoM). In the theory of IoM's, it is assumed that the true pdf/pmf p^* of interest is such that $p^*(x) \in [\ell(x), u(x)]$, for all x , where ℓ and u are the lower and upper pdf/pmf's, respectively. In turn, (Coolen 1992; Wasserman 1992) remark how an IoM can be thought of as a neighborhood of a probability measure, which is itself a credal set. This heuristic connection between $[\underline{\Phi}(x), \overline{\Phi}(x)]$ and credal sets explains why $\mathcal{U}(\cdot)$ satisfying (1)-(4) is an indicator of it being a good uncertainty measure.

We conclude the remark by noting the following. Fix $\beta, \lambda > 0$, and pick $x, x' \in \mathcal{X}$ such that $\underline{\Phi}(x') < \underline{\Phi}(x)$ and $\overline{\Phi}(x') > \overline{\Phi}(x)$. Let $A = \{\underline{\Phi}(x) - \lambda\beta \leq y \leq \overline{\Phi}(x) + \lambda\beta\}$ and $A' = \{\underline{\Phi}(x') - \lambda\beta \leq y \leq \overline{\Phi}(x') + \lambda\beta\}$, and note that $A, A' \in \mathcal{A}_{\mathcal{Y}}$. Then,

$$\begin{aligned} \mathbb{E}_X [\overline{P}_{Y|X}(A')] - \mathbb{E}_X [P_{Y|X}(A')] \\ \leq \mathbb{E}_X [\overline{P}_{Y|X}(A)] - \mathbb{E}_X [P_{Y|X}(A)]. \end{aligned}$$

This is an immediate result of the monotonicity of upper and lower probabilities (Cerreia-Vioglio, Maccheroni, and Marinacci 2015, Section 2.1) and Corollary 4. We can say that, for any given $A^* \in \mathcal{A}_{\mathcal{Y}}$, the difference $\mathbb{E}_X[\overline{P}_{Y|X}(A^*)] - \mathbb{E}_X[P_{Y|X}(A^*)]$ represents the *individual epistemic uncertainty* of A^* (Caprio et al. 2022, Section 4). The result, then, is intuitive. For elements x whose associated network uncertainty $\mathcal{U}(x)$ is high, we have that the individual epistemic uncertainty of the induced set $\{\underline{\Phi}(x) - \lambda\beta \leq y \leq \overline{\Phi}(x) + \lambda\beta\}$ in \mathcal{Y} is low. That because the interval $[\underline{\Phi}(x) - \lambda\beta, \overline{\Phi}(x) + \lambda\beta]$ is wide, so there is a higher chance for the true output y to lie in it.

6 Experimental Evaluation

In this section, we present an experimental evaluation of our INN-based probabilistic guarantees. For our case studies, we consider closed-loop interactions of a black-box simulator with a control policy obtained with reinforcement learning. The goal is to determine a lower bound on the expected performance score and to construct a set of distributions for which the guarantee holds. Here, the performance score is an average over time of the rewards obtained by executing the policy. Our approach evaluates systems of higher dimension (> 10) and can satisfy coverage guarantees.

Environments Here we consider the complete set of 10 environments from the Mujoco tasks in the OpenAI gymnasium control suite (Brockman et al. 2016). The control policy for the environments are trained using DDPG algorithm (refer to Appendix B for details). We select the initialization of each environment using the provided API. The subsequent evolution is deterministic. We simulate the environments until termination and compute the temporal average of the reward as $R_{avg} = \frac{1}{T} \sum_{i=1}^T r_i$. Here, r_i is the reward at time step i , and T is the duration of the episode. In our experiments we set the confidence parameter to 95% by choosing $\lambda = 20$. For the INN, we select $k = 3$ DNNs. Each DNN is a 2 layer feedforward neural network with a width of 50 and ReLU activation. The width of the exploration set δ is set to 0.05, which is half of the full range picked by the Mujoco suite developers. The number of iterations of active learning is set to $M = 20$. We draw $N = 200$ samples each time we sample a local region (Algorithm 1, Line 6).

Computing Lower Bounds on Performance We wish to compute the lower bound ϵ on the performance function R_{avg} . The bounds $(\underline{\Phi}(x) - \lambda\beta)$ computed using Algorithm 2 are presented in Table 1. The total number of points used for training the INN is $4.2k$ samples. We empirically check the validity of the lower bounds proposed by the INN, by

Environment	\mathcal{X} Dim	$\beta = 10^{-4}$		$\beta = 10^{-3}$		$\beta = 10^{-2}$	
		Lower Bound	Cov. (%)	Lower Bound	Cov. (%)	Lower Bound	Cov. (%)
Ant	29	-1.29	99.9	-1.58	100	-0.98	99.3
Half-Cheetah	18	3.97	100	9.1	99.8	8.71	99.8
Hopper	12	1.4	99.9	1.45	99.8	1.46	99.8
Humanoid	47	4.72	100	4.5	100	4.99	99.1
Humanoid-Standup	47	121.2	99.7	100	100	143.6	99.4
Inverted Double Pend.	6	6.4	100	9.1	100	8.94	100
Inverted Pendulum	4	0.64	100	0.98	100	0.8	100
Reacher	8	-0.08	100	-0.1	100	-0.28	100
Swimmer	10	0.13	100	0.12	100	-0.06	100
Walker2d	18	0.62	99.5	0.35	99.7	0.25	99.7

Table 1: We estimate the lower limit on R_{avg} using the proposed INN method, and compare it with $20k$ samples drawn uniformly from the whole initial set \mathcal{X}_0 . We observe that the fraction of samples which satisfy the estimated lower bounds (i.e., coverage ‘‘Cov.’’) are well above the 95% target. Here, \mathcal{X} denotes the input space.

drawing $20k$ samples uniformly from the initial set \mathcal{X}_0 . We compute the fraction of times the simulations return a value above the INN proposed lower limit from this sample set. This fraction is presented in Table 1, as percentage coverage. The same experiment is repeated for different values of β . We observe that for all the environments, more than 99% of the samples return R_{avg} values above the predicted score.

Comparison with Conformal Prediction We compare our method to inductive conformal prediction (ICP), a variant of CP designed to improve computational efficiency (Papadopoulos et al. 2002; Vovk, Gammerman, and Shafer 2005). Given a model f trained on set $\mathcal{X}_{tr} \sim P_{\mathcal{X}}$, a calibration set $\mathcal{X}_{cal} \sim P_{\mathcal{X}}$, a non-conformity score function s , for confidence level $\alpha \in (0, 1)$, ICP produces a prediction region $C(x_{te})$ such that $P(y_{te} \in C(x_{te})) \geq 1 - \alpha$. The non-conformity score captures the quality of a model’s prediction (e.g., $s(x, y) = |y - f(x)|$ for an input x and its ground-truth target y). In our experiments, the final set of explored states \mathcal{X}_e is divided into a training and calibration set for CP ($\mathcal{X}_e = \mathcal{X}_{tr} \cup \mathcal{X}_{cal}$). The CP prediction intervals capture the uncertainty in the estimates of the performance R_{avg} . Generally, CP algorithms can be restrictive as they typically require that the test data be drawn from the same distribution as the training data (i.e., $x_{te} \sim P_{\mathcal{X}}$). This can be difficult to guarantee in practice. Therefore in our experiments, we compare the quality of the prediction intervals produced by our INN model to those of ICP in terms of prediction coverage and size. We evaluate the methods under two settings:

- In-distribution Evaluation:** Test samples are drawn from a uniform distribution matching the training distribution for INNs and ICP. The 95% confidence regions proposed by ICP are compared to the INN intervals computed as $[\Phi(x) - \lambda\beta, \Phi(x) + \lambda\beta]$.
- Out-of-distribution Evaluation:** Test samples are drawn from a uniform distribution NOT matching the training distribution. Note, that the training distribution is a mixture of uniform distributions over specific inter-

vals in the input space. The testing samples are sampled uniformly over the entire input space.

The results of in-distribution evaluation are presented in Table 2. We observe that the prediction regions proposed by the INN have a higher coverage rate, while the coverage guarantees for CP do not hold precisely in some cases. However, this comes at the cost of larger width of the INN intervals for some cases.

For the out-of-distribution evaluation, in order for the guarantees of CP to hold, the test distribution cannot be drawn uniformly from the entire input space \mathcal{X}_0 . In comparison, as discussed in Section 4, the uniform distribution over the entire set is covered in our family of distributions. The ramifications of this can be observed in Table 3. The prediction regions of CP violate the coverage guarantees while intervals proposed with our INN method has a coverage rate above 95%.

Environment	\mathcal{X} Dim	Conformal Prediction		INN (ours)	
		Coverage (%)	Interval Size	Coverage (%)	Interval Size
Ant	29	93	3.2	99	4.2
Half-Cheetah	18	93	4.9×10^{-1}	100	3
Hopper	12	97	2.9	100	2.2
Humanoid	47	97	2.7	100	3
Humanoid-Standup	47	96	143	99	260
Inverted Double Pend.	6	95	6.7×10^{-3}	100	5.1×10^{-2}
Inverted Pendulum	4	95	1.2×10^{-3}	100	4.1×10^{-2}
Reacher	8	93	3.3×10^{-2}	100	7.6×10^{-2}
Swimmer	10	93	2.8×10^{-3}	100	4.9×10^{-2}
Walker2d	18	95	5.2	99	5.8

Table 2: We compare the coverage rates and size of prediction regions between an INN and CP for $\beta = 10^{-3}$ when the test samples are in-distribution. \mathcal{X} denotes the input space. The interval size of the INN is an average value across the samples.

Environment	\mathcal{X} Dim	Conformal Prediction		INN (ours)	
		Coverage (%)	Interval Size	Coverage (%)	Interval Size
Ant	29	94	3.2	100	4.3
Half-Cheetah	18	93	4.9×10^{-1}	100	1.9
Hopper	12	97	2.9	100	2.5
Humanoid	47	98	2.7	99	2.8
Humanoid-Standup	47	95	143	100	262
Inverted Double Pend.	6	94	6.7×10^{-3}	100	5.1×10^{-2}
Inverted Pendulum	4	100	1.2×10^{-3}	100	4.2×10^{-2}
Reacher	8	91	3.3×10^{-2}	100	8.5×10^{-2}
Swimmer	10	92	2.8×10^{-3}	100	5×10^{-2}
Walker2d	18	94	5.2	99	5.2

Table 3: We compare the coverage rates and size of prediction regions between an INN and CP for $\beta = 10^{-3}$ when the test samples are out-of-distribution. \mathcal{X} denotes the input space. The interval size of the INN is an average value across the samples.

Ablations We perform further ablations on different values of $\beta\{10^{-2}, 10^{-4}\}$, presented in Table 4, and Table 5 in Appendix B. We observe similar trends wherein the INN has better coverage guarantees but is more conservative.

Conclusion

In this paper, we show that uncertainty quantification can step outside of the limitations of being restricted to a single distribution. We validate this claim experimentally by demonstrating this over state-of-the-art high-dimensional case studies commonly explored in the reinforcement learning literature. The bounds estimated hold in both the in-distribution and out-of-distribution cases. In the future, we plan to explore more efficient ways to perform active learning that can avoid expensive queries to a neural-network verification tool.

References

- Abellán, J.; and Klir, G. J. 2005. Additivity of uncertainty measures on credal sets. *International Journal of General Systems*, 34(6): 691–713.
- Alasmari, N.; Calinescu, R.; Paterson, C.; and Mirandola, R. 2022. Quantitative verification with adaptive uncertainty reduction. *Journal of Systems and Software*, 188: 111275.
- Aoude, G. S.; Luders, B. D.; Joseph, J. M.; Roy, N.; and How, J. P. 2013. Probabilistically safe motion planning to avoid dynamic obstacles with uncertain motion patterns. *Autonomous Robots*, 35(1): 51–76.
- Ashok, P.; Hashemi, V.; Křetínský, J.; and Mohr, S. 2020. DeepAbstract: Neural Network Abstraction for Accelerating Verification. In Hung, D. V.; and Sokolsky, O., eds., *Automated Technology for Verification and Analysis*, Lecture Notes in Computer Science, 92–107. Cham: Springer International Publishing. ISBN 978-3-030-59152-6.
- Bansal, S.; Ghosh, S.; Sangiovanni-Vincentelli, A.; Seshia, S. A.; and Tomlin, C. J. 2018. Context-Specific Validation of Data-Driven Models. *arXiv:1802.04929 [cs]*. ArXiv: 1802.04929.
- Brockman, G.; Cheung, V.; Pettersson, L.; Schneider, J.; Schulman, J.; Tang, J.; and Zaremba, W. 2016. OpenAI Gym. ArXiv:1606.01540 [cs].
- Burbidge, R.; Rowland, J. J.; and King, R. D. 2007. Active Learning for Regression Based on Query by Committee. In Yin, H.; Tino, P.; Corchado, E.; Byrne, W.; and Yao, X., eds., *Intelligent Data Engineering and Automated Learning - IDEAL 2007*, 209–218. Berlin, Heidelberg: Springer Berlin Heidelberg. ISBN 978-3-540-77226-2.
- Cairoli, F.; Bortolussi, L.; and Paoletti, N. 2021. Neural Predictive Monitoring Under Partial Observability. In Feng, L.; and Fisman, D., eds., *Runtime Verification*, 121–141. Cham: Springer International Publishing. ISBN 978-3-030-88494-9.
- Caprio, M.; Dutta, S.; Ivanov, R.; Jang, K.; Lin, V.; Sokolsky, O.; and Lee, I. 2022. Imprecise Bayesian Neural Networks. *Submitted to AAI 2023*.
- Caprio, M.; Sale, Y.; Hüllermeier, E.; and Lee, I. 2023. A Novel Bayes’ Theorem for Upper Probabilities. *Available at arXiv:2307.06831*.
- Cardelli, L.; Kwiatkowska, M.; Laurenti, L.; Paoletti, N.; Patane, A.; and Wicker, M. 2019. Statistical Guarantees for the Robustness of Bayesian Neural Networks. 5693–5700.
- Castaneda, F.; Choi, J. J.; Zhang, B.; Tomlin, C. J.; and Sreenath, K. 2021. Pointwise Feasibility of Gaussian Process-based Safety-Critical Control under Model Uncertainty. In *2021 60th IEEE Conference on Decision and Control (CDC)*, 6762–6769. ISSN: 2576-2370.
- Cerreia-Vioglio, S.; Maccheroni, F.; and Marinacci, M. 2015. Ergodic theorems for lower probabilities. *Proceedings of the American Mathematical Society*, 144: 3381–3396.
- Chakraborty, K.; and Bansal, S. 2023. Discovering Closed-Loop Failures of Vision-Based Controllers via Reachability Analysis. *IEEE Robotics and Automation Letters*, 8(5): 2692–2699. Conference Name: IEEE Robotics and Automation Letters.
- Cleaveland, M.; Lindemann, L.; Ivanov, R.; and Pappas, G. J. 2022. Risk verification of stochastic systems with neural network controllers. *Artificial Intelligence*, 313: 103782.
- Coolen, F. P. A. 1992. Imprecise highest density regions related to intervals of measures. *Memorandum COSOR*, 9254.
- Corso, A.; Moss, R.; Koren, M.; Lee, R.; and Kochenderfer, M. 2022. A Survey of Algorithms for Black-Box Safety Validation of Cyber-Physical Systems. *Journal of Artificial Intelligence Research*, 72: 377–428.
- Cubuktepe, M.; Jansen, N.; Junges, S.; Katoen, J.-P.; and Topcu, U. 2020. Scenario-Based Verification of Uncertain MDPs. In *Tools and Algorithms for the Construction and Analysis of Systems*, Lecture Notes in Computer Science, 287–305. Cham: Springer International Publishing. ISBN 978-3-030-45190-5.
- Denoeux, T. 2022. An Evidential Neural Network Model for Regression Based on Random Fuzzy Numbers. *Available at arXiv:2208.00647*.
- Divband Soorati, M.; Gerding, E. H.; Marchioni, E.; Naumov, P.; Norman, T. J.; Ramchurn, S. D.; Rastegari, B.; Sobey, A.; Stein, S.; Tarpore, D.; Yazdanpanah, V.; Zhang, J.; Albrecht, S. V.; and Woolridge, M. 2022. From intelligent agents to trustworthy human-centred multiagent systems. *AI Communications*, 35(4): 443–457.
- Dreossi, T.; Fremont, D. J.; Ghosh, S.; Kim, E.; Ravanbakhsh, H.; Vazquez-Chanlatte, M.; and Seshia, S. A. 2019. VERIFAI: A Toolkit for the Design and Analysis of Artificial Intelligence-Based Systems. *arXiv:1902.04245 [cs]*. ArXiv: 1902.04245.
- Du, X.; Wang, Z.; Cai, M.; and Li, Y. 2022. VOS: Learning What You Don’t Know by Virtual Outlier Synthesis.
- Dutta, S.; Chen, X.; Jha, S.; Sankaranarayanan, S.; and Tiwari, A. 2019. Sherlock - A Tool for Verification of Neural Network Feedback Systems: Demo Abstract. HSCC ’19, 262–263. New York, NY, USA: Association for Computing Machinery. ISBN 9781450362825.
- Dutta, S.; Chen, X.; and Sankaranarayanan, S. 2019. Reachability analysis for neural feedback systems using regressive polynomial rule inference. In *Proceedings of the 22nd ACM International Conference on Hybrid Systems: Computation and Control*, HSCC ’19, 157–168. New York, NY, USA: Association for Computing Machinery. ISBN 978-1-4503-6282-5.

- Dutta, S.; Jha, S.; Sankaranarayanan, S.; and Tiwari, A. 2018a. Output Range Analysis for Deep Feedforward Neural Networks. In Dutle, A.; Muñoz, C.; and Narkawicz, A., eds., *NASA Formal Methods*, Lecture Notes in Computer Science, 121–138. Cham: Springer International Publishing. ISBN 978-3-319-77935-5.
- Dutta, S.; Jha, S.; Sankaranarayanan, S.; and Tiwari, A. 2018b. Output Range Analysis for Deep Feedforward Neural Networks. In Dutle, A.; Muñoz, C.; and Narkawicz, A., eds., *NASA Formal Methods*, 121–138. Cham: Springer International Publishing. ISBN 978-3-319-77935-5.
- Elboher, Y. Y.; Gottschlich, J.; and Katz, G. 2019. An Abstraction-Based Framework for Neural Network Verification. ArXiv: 1910.14574.
- Farid, A.; Veer, S.; and Majumdar, A. 2022. Task-Driven Out-of-Distribution Detection with Statistical Guarantees for Robot Learning. In *Proceedings of the 5th Conference on Robot Learning*, 970–980. PMLR. ISSN: 2640-3498.
- Fazlyab, M.; Morari, M.; and Pappas, G. J. 2019. Probabilistic Verification and Reachability Analysis of Neural Networks via Semidefinite Programming. In *2019 IEEE 58th Conference on Decision and Control (CDC)*, 2726–2731. ISSN: 2576-2370.
- Gehr, T.; Mirman, M.; Drachler-Cohen, D.; Tsankov, P.; Chaudhuri, S.; and Vechev, M. 2018. AI2: Safety and Robustness Certification of Neural Networks with Abstract Interpretation. In *2018 IEEE Symposium on Security and Privacy (SP)*, 3–18.
- Gong, R.; and Meng, X.-L. 2021. Judicious judgment meets unsettling updating: dilation, sure loss, and Simpson’s paradox. *Statistical Science*, 36(2): 169–190.
- Guo, C.; Pleiss, G.; Sun, Y.; and Weinberger, K. Q. 2017. On calibration of modern neural networks. In *Proceedings of the 34th International Conference on Machine Learning - Volume 70*, ICML’17, 1321–1330. Sydney, NSW, Australia: JMLR.org.
- Gupta, C.; Podkopaev, A.; and Ramdas, A. 2022. Distribution-free binary classification: prediction sets, confidence intervals and calibration. *arXiv:2006.10564 [cs, math, stat]*. ArXiv: 2006.10564.
- Huber, P. J.; and Ronchetti, E. M. 2009. *Robust statistics*. Wiley Series in Probability and Statistics. Hoboken, New Jersey : Wiley, 2nd edition.
- Ivanov, R.; Carpenter, T.; Weimer, J.; Alur, R.; Pappas, G.; and Lee, I. 2021. Verisig 2.0: Verification of Neural Network Controllers Using Taylor Model Preconditioning. In *Computer Aided Verification*, 249–262. Cham: Springer International Publishing. ISBN 978-3-030-81685-8.
- Jiroušek, R.; and Shenoy, P. P. 2018. A new definition of entropy of belief functions in the Dempster–Shafer theory. *International Journal of Approximate Reasoning*, 92: 49–65.
- Katz, G.; Barrett, C.; Dill, D.; Julian, K.; and Kochenderfer, M. 2017. Reluplex: An Efficient SMT Solver for Verifying Deep Neural Networks. *arXiv:1702.01135 [cs]*. ArXiv: 1702.01135.
- Ladner, T.; and Althoff, M. 2023. Automatic Abstraction Refinement in Neural Network Verification using Sensitivity Analysis. In *Proceedings of the 26th ACM International Conference on Hybrid Systems: Computation and Control*, HSCC ’23, 1–13. New York, NY, USA: Association for Computing Machinery. ISBN 9798400700330.
- Lakshminarayanan, B.; Pritzel, A.; and Blundell, C. 2017. Simple and scalable predictive uncertainty estimation using deep ensembles. In *Proceedings of the 31st International Conference on Neural Information Processing Systems*, NIPS’17, 6405–6416. Red Hook, NY, USA: Curran Associates Inc. ISBN 978-1-5108-6096-4.
- Larsen, K. G.; and Legay, A. 2014. Statistical Model Checking Past, Present, and Future. In Margaria, T.; and Steffen, B., eds., *Leveraging Applications of Formal Methods, Verification and Validation. Specialized Techniques and Applications*, Lecture Notes in Computer Science, 135–142. Berlin, Heidelberg: Springer. ISBN 978-3-662-45231-8.
- Lew, T.; Janson, L.; Bonalli, R.; and Pavone, M. 2022. A Simple and Efficient Sampling-based Algorithm for General Reachability Analysis. In Firoozi, R.; Mehr, N.; Yel, E.; Antonova, R.; Bohg, J.; Schwager, M.; and Kochenderfer, M., eds., *Proceedings of The 4th Annual Learning for Dynamics and Control Conference*, volume 168 of *Proceedings of Machine Learning Research*, 1086–1099. PMLR.
- Lindemann, L.; Qin, X.; Deshmukh, J. V.; and Pappas, G. J. 2023. Conformal Prediction for STL Runtime Verification. In *Proceedings of the ACM/IEEE 14th International Conference on Cyber-Physical Systems (with CPS-IoT Week 2023)*, ICCPS ’23, 142–153. New York, NY, USA: Association for Computing Machinery. ISBN 9798400700361.
- Liu, H.; Ong, Y.-S.; Shen, X.; and Cai, J. 2020. When Gaussian Process Meets Big Data: A Review of Scalable GPs. *IEEE Transactions on Neural Networks and Learning Systems*, 31(11): 4405–4423. Conference Name: IEEE Transactions on Neural Networks and Learning Systems.
- Luo, R.; Zhao, S.; Kuck, J.; Ivanovic, B.; Savarese, S.; Schmerling, E.; and Pavone, M. 2023. Sample-Efficient Safety Assurances Using Conformal Prediction. In LaValle, S. M.; O’Kane, J. M.; Otte, M.; Sadigh, D.; and Tokekar, P., eds., *Algorithmic Foundations of Robotics XV*, 149–169. Cham: Springer International Publishing. ISBN 978-3-031-21090-7.
- Michelmore, R.; Wicker, M.; Laurenti, L.; Cardelli, L.; Gal, Y.; and Kwiatkowska, M. 2020. Uncertainty Quantification with Statistical Guarantees in End-to-End Autonomous Driving Control. *2020 IEEE International Conference on Robotics and Automation (ICRA)*.
- Minderer, M.; Djolonga, J.; Romijnders, R.; Hubis, F.; Zhai, X.; Houlsby, N.; Tran, D.; and Lucic, M. 2021. Revisiting the Calibration of Modern Neural Networks. In *Advances in Neural Information Processing Systems*, volume 34, 15682–15694. Curran Associates, Inc.

- Mitra, S. 2021. *Verifying Cyber-Physical Systems: A Path to Safe Autonomy*. Cambridge, Massachusetts: The MIT Press. ISBN 978-0-262-04480-6.
- Moss, R. J.; Kochenderfer, M. J.; Gariel, M.; and Dubois, A. 2023. Bayesian Safety Validation for Black-Box Systems. In *Conference proceedings of the 2023 AIAA AVIATION Forum*. ArXiv:2305.02449 [cs, stat].
- Muthali, A.; Shen, H.; Deglurkar, S.; Lim, M. H.; Roelofs, R.; Faust, A.; and Tomlin, C. 2023. Multi-Agent Reachability Calibration with Conformal Prediction. arXiv:2304.00432.
- Oala, L.; Heiß, C.; MacDonald, J.; März, M.; Samek, W.; and Kutyniok, G. 2020. Interval Neural Networks: Uncertainty Scores. *ArXiv*, abs/2003.11566.
- Papadopoulos, H.; Proedrou, K.; Vovk, V.; and Gammerman, A. 2002. Inductive confidence machines for regression. In *Machine Learning: ECML 2002: 13th European Conference on Machine Learning Helsinki, Finland, August 19–23, 2002 Proceedings 13*, 345–356. Springer.
- Park, S.; Li, S.; Bastani, O.; and Lee, I. 2021. PAC Confidence Predictions for Deep Neural Network Classifiers. *ICLR*.
- Pearce, T.; Brintrup, A.; Zaki, M.; and Neely, A. 2018. High-Quality Prediction Intervals for Deep Learning: A Distribution-Free, Ensembled Approach. In *Proceedings of the 35th International Conference on Machine Learning*, 4075–4084. PMLR. ISSN: 2640-3498.
- Petrov, A.; Fang, C.; Pham, K. M.; Eng, Y. H.; Ming Fu, J. G.; and Pendleton, S. D. 2022. HiddenGems: Efficient safety boundary detection with active learning. In *2022 IEEE/RSJ International Conference on Intelligent Robots and Systems (IROS)*, 5147–5154. ISSN: 2153-0866.
- Qin, X.; Xian, Y.; Zutshi, A.; Fan, C.; and Deshmukh, J. 2021. Statistical Verification of Autonomous Systems using Surrogate Models and Conformal Inference. In *Proc. of ICCPS'22*. ArXiv: 2004.00279.
- Rasmussen, C. E.; and Williams, C. K. I. 2005. *Gaussian Processes for Machine Learning*. Cambridge, Mass: The MIT Press. ISBN 978-0-262-18253-9.
- Seshia, S. A.; Sadigh, D.; and Sastry, S. S. 2022. Toward verified artificial intelligence. *Communications of the ACM*, 65(7): 46–55.
- Seung, H. S.; Opper, M.; and Sompolinsky, H. 1992. Query by committee. In *Proceedings of the fifth annual workshop on Computational learning theory*, COLT '92, 287–294. New York, NY, USA: Association for Computing Machinery. ISBN 978-0-89791-497-0.
- Shafer, G.; and Vovk, V. 2008. A Tutorial on Conformal Prediction. *J. Mach. Learn. Res.*, 9: 371–421.
- Sidrane, C.; Maleki, A.; Irfan, A.; and Kochenderfer, M. J. 2022. OVERT: an algorithm for safety verification of neural network control policies for nonlinear systems. *The Journal of Machine Learning Research*, 23(1): 117:5090–117:5134.
- Sinha, R.; Sharma, A.; Banerjee, S.; Lew, T.; Luo, R.; Richards, S. M.; Sun, Y.; Schmerling, E.; and Pavone, M. 2022. A System-Level View on Out-of-Distribution Data in Robotics.
- Smith, R. C. 2013. *Uncertainty Quantification: Theory, Implementation, and Applications*. SIAM. ISBN 978-1-61197-321-1. Google-Books-ID: 4c1GAgAAQBAJ.
- Song, J.; Lyu, D.; Zhang, Z.; Wang, Z.; Zhang, T.; and Ma, L. 2022. When Cyber-Physical Systems Meet AI: A Benchmark, an Evaluation, and a Way Forward. In *Proceedings of the 44th International Conference on Software Engineering: Software Engineering in Practice*, 343–352. ArXiv:2111.04324 [cs].
- Sullivan. 2015. *Introduction to Uncertainty Quantification*. New York, NY: Springer, 1st ed. 2015 edition edition. ISBN 978-3-319-23394-9.
- Tomar, M.; Mishra, U. A.; Zhang, A.; and Taylor, M. E. 2022. Learning Representations for Pixel-based Control: What Matters and Why? *Transactions on Machine Learning Research*.
- Tran, H.-D.; Yang, X.; Manzananas Lopez, D.; Musau, P.; Nguyen, L. V.; Xiang, W.; Bak, S.; and Johnson, T. T. 2020. NNV: The Neural Network Verification Tool for Deep Neural Networks and Learning-Enabled Cyber-Physical Systems. In *Computer Aided Verification*.
- Tretiak, K.; Schollmeyer, G.; and Ferson, S. 2022. Neural network model for imprecise regression with interval dependent variables. Available at arXiv:2206.02467.
- Troffaes, M. C.; and de Cooman, G. 2014. *Lower Previsions*. Chichester, United Kingdom : John Wiley and Sons.
- Vovk, V.; Gammerman, A.; and Shafer, G. 2005. *Algorithmic Learning in a Random World*. New York: Springer, 2005 edition edition. ISBN 978-0-387-00152-4.
- Walley, P. 1991. *Statistical Reasoning with Imprecise Probabilities*, volume 42 of *Monographs on Statistics and Applied Probability*. London : Chapman and Hall.
- Wang, Y.; Zarei, M.; Bonakdarpoor, B.; and Pajic, M. 2021. Probabilistic conformance for cyber-physical systems. In *Proceedings of the ACM/IEEE 12th International Conference on Cyber-Physical Systems, ICCPS '21*, 55–66. New York, NY, USA: Association for Computing Machinery. ISBN 978-1-4503-8353-0.
- Wasserman, L. 1992. Recent methodological advances in robust Bayesian inference. *Bayesian statistics*, 4: 483–502.
- Wasserman, L. A.; and Kadane, J. B. 1990. Bayes' Theorem for Choquet Capacities. *The Annals of Statistics*, 18(3): 1328–1339.
- Wicker, M.; Laurenti, L.; Patane, A.; and Kwiatkowska, M. 2020. Probabilistic Safety for Bayesian Neural Networks. In *Proceedings of the 36th Conference on Uncertainty in Artificial Intelligence (UAI)*, 1198–1207. PMLR. ISSN: 2640-3498.
- Zarei, M.; Wang, Y.; and Pajic, M. 2020. Statistical verification of learning-based cyber-physical systems. In *Proceedings of the 23rd International Conference on Hybrid Systems: Computation and Control, HSCC '20*, 1–7. New York, NY, USA: Association for Computing Machinery. ISBN 978-1-4503-7018-9.

Zhang, Z.; Lyu, D.; Arcaini, P.; Ma, L.; Hasuo, I.; and Zhao, J. 2023. FalsifAI: Falsification of AI-Enabled Hybrid Control Systems Guided by Time-Aware Coverage Criteria. *IEEE Transactions on Software Engineering*, 49(4): 1842–1859. Conference Name: IEEE Transactions on Software Engineering.

A Appendix

Proofs

Proof of Theorem 3. Let us write the partial derivative of $\mathcal{L}(\underline{\Phi}, \bar{\Phi})$ with respect to $\bar{\Phi}(x)$

$$\frac{\partial \mathcal{L}(\underline{\Phi}, \bar{\Phi})}{\partial \bar{\Phi}(x)} = \frac{\partial}{\partial \bar{\Phi}(x)} \sup_{P_X \in \mathcal{P}_X} \int_{\mathcal{X}} [\bar{\mathbb{E}}_{Y|X}(\bar{m}^2) + \bar{\mathbb{E}}_{Y|X}(\underline{m}^2) + \beta (\bar{\Phi}(x) - \underline{\Phi}(x))] P_X(\mathrm{d}x). \quad (4)$$

Since we assumed \mathcal{P}_X to be compact, then there is $\tilde{P}_X \in \mathcal{P}_X$ such that

$$\begin{aligned} & \sup_{P_X \in \mathcal{P}_X} \int_{\mathcal{X}} [\bar{\mathbb{E}}_{Y|X}(\bar{m}^2) + \bar{\mathbb{E}}_{Y|X}(\underline{m}^2) + \beta (\bar{\Phi}(x) - \underline{\Phi}(x))] P_X(\mathrm{d}x) \\ &= \int_{\mathcal{X}} [\bar{\mathbb{E}}_{Y|X}(\bar{m}^2) + \bar{\mathbb{E}}_{Y|X}(\underline{m}^2) + \beta (\bar{\Phi}(x) - \underline{\Phi}(x))] \tilde{P}_X(\mathrm{d}x). \end{aligned}$$

Then, (4) can be rewritten as

$$\frac{\partial \mathcal{L}(\underline{\Phi}, \bar{\Phi})}{\partial \bar{\Phi}(x)} = \frac{\partial}{\partial \bar{\Phi}(x)} \int_{\mathcal{X}} [\bar{\mathbb{E}}_{Y|X}(\bar{m}^2) + \bar{\mathbb{E}}_{Y|X}(\underline{m}^2) + \beta (\bar{\Phi}(x) - \underline{\Phi}(x))] \tilde{P}_X(\mathrm{d}x).$$

From Leibniz integral rule and the additivity of the derivative operator, then, we can write

$$\begin{aligned} \frac{\partial \mathcal{L}(\underline{\Phi}, \bar{\Phi})}{\partial \bar{\Phi}(x)} &= \int_{\mathcal{X}} \frac{\partial}{\partial \bar{\Phi}(x)} [\bar{\mathbb{E}}_{Y|X}(\bar{m}^2) + \bar{\mathbb{E}}_{Y|X}(\underline{m}^2) + \beta (\bar{\Phi}(x) - \underline{\Phi}(x))] \tilde{P}_X(\mathrm{d}x) \\ &= \int_{\mathcal{X}} \frac{\partial}{\partial \bar{\Phi}(x)} \bar{\mathbb{E}}_{Y|X}(\bar{m}^2) + \frac{\partial}{\partial \bar{\Phi}(x)} \bar{\mathbb{E}}_{Y|X}(\underline{m}^2) + \frac{\partial}{\partial \bar{\Phi}(x)} [\beta (\bar{\Phi}(x) - \underline{\Phi}(x))] \tilde{P}_X(\mathrm{d}x). \end{aligned} \quad (5)$$

Since we assumed that $\mathcal{P}_{Y|X}$ to be compact, there are $P_{Y|X}^*, P_{Y|X}^{**}$ in $\mathcal{P}_{Y|X}$, possibly different from each other, such that

$$\begin{aligned} \bar{\mathbb{E}}_{Y|X}(\bar{m}^2) &:= \sup_{P_{Y|X} \in \mathcal{P}_{Y|X}} \int_{\mathcal{Y}} \max(y - \bar{\Phi}(x), 0)^2 P_{Y|X}(\mathrm{d}y) \\ &= \int_{\mathcal{Y}} \max(y - \bar{\Phi}(x), 0)^2 P_{Y|X}^*(\mathrm{d}y) =: \mathbb{E}_{Y|X}^*(\bar{m}^2) \end{aligned}$$

and

$$\begin{aligned} \bar{\mathbb{E}}_{Y|X}(\underline{m}^2) &:= \sup_{P_{Y|X} \in \mathcal{P}_{Y|X}} \int_{\mathcal{Y}} \max(\underline{\Phi}(x) - y, 0)^2 P_{Y|X}(\mathrm{d}y) \\ &= \int_{\mathcal{Y}} \max(\underline{\Phi}(x) - y, 0)^2 P_{Y|X}^{**}(\mathrm{d}y) =: \mathbb{E}_{Y|X}^{**}(\underline{m}^2). \end{aligned}$$

So we can rewrite (5) as

$$\begin{aligned} \frac{\partial \mathcal{L}(\underline{\Phi}, \bar{\Phi})}{\partial \bar{\Phi}(x)} &= \int_{\mathcal{X}} \frac{\partial}{\partial \bar{\Phi}(x)} \mathbb{E}_{Y|X}^*(\bar{m}^2) + \frac{\partial}{\partial \bar{\Phi}(x)} \mathbb{E}_{Y|X}^{**}(\underline{m}^2) + \frac{\partial}{\partial \bar{\Phi}(x)} [\beta (\bar{\Phi}(x) - \underline{\Phi}(x))] \tilde{P}_X(\mathrm{d}x) \\ &= (-2) \int_{\mathcal{X}} \mathbb{E}_{Y|X}^*(\bar{m}) \tilde{P}_X(\mathrm{d}x) + \beta. \end{aligned} \quad (6)$$

Assuming that $\mathcal{L}(\underline{\Phi}, \bar{\Phi})$ is optimized, we have that $\partial \mathcal{L}(\underline{\Phi}, \bar{\Phi}) / \partial \bar{\Phi}(x) = 0$, which by (6) holds if and only if

$$\frac{\beta}{2} = \int_{\mathcal{X}} \mathbb{E}_{Y|X}^*(\bar{m}) \tilde{P}_X(\mathrm{d}x) = \sup_{P_X \in \mathcal{P}_X} \int_{\mathcal{X}} \bar{\mathbb{E}}_{Y|X}(\bar{m}) P_X(\mathrm{d}x). \quad (7)$$

Analogously, we have that

$$\frac{\beta}{2} = \int_{\mathcal{X}} \mathbb{E}_{Y|X}^{**}(\underline{m}) \tilde{P}_X(\mathrm{d}x) = \sup_{P_X \in \mathcal{P}_X} \int_{\mathcal{X}} \bar{\mathbb{E}}_{Y|X}(\underline{m}) P_X(\mathrm{d}x). \quad (8)$$

Let now $h_1(\zeta) := \max(\zeta - \bar{\Phi}(x), 0)$ and $h_2(\zeta) := \max(\zeta + \underline{\Phi}(x), 0)$. By Markov's inequality, we have that for all $P_{Y|X} \in \mathcal{P}_{Y|X}$,

$$P_{Y|X}(y \geq \bar{\Phi}(x) + \lambda\beta) \leq \frac{\mathbb{E}_{Y|X}[h_1(y)]}{h_1(\bar{\Phi}(x) + \lambda\beta)} = \frac{\mathbb{E}_{Y|X}(\bar{m})}{\lambda\beta}.$$

This implies that

$$\bar{P}_{Y|X}(y \geq \bar{\Phi}(x) + \lambda\beta) \leq \frac{\bar{\mathbb{E}}_{Y|X}(\bar{m})}{\lambda\beta}. \quad (9)$$

Similarly,

$$\bar{P}_{Y|X}(y \leq \underline{\Phi}(x) - \lambda\beta) \leq \frac{\bar{\mathbb{E}}_{Y|X}(\underline{m})}{\lambda\beta}. \quad (10)$$

Recall that $A = \{\underline{\Phi}(x) - \lambda\beta \leq y \leq \bar{\Phi}(x) + \lambda\beta\}$; then, we have the following

$$\mathbb{E}_X [P_{Y|X}(A)] = \mathbb{E}_X [1 - \bar{P}_{Y|X}(A^c)] \quad (11)$$

$$\begin{aligned} &= \inf_{P_X \in \mathcal{P}_X} \int_{\mathcal{X}} [1 - \bar{P}_{Y|X}(A^c)] P_X(\mathrm{d}x) \\ &= \inf_{P_X \in \mathcal{P}_X} \left[1 - \int_{\mathcal{X}} \bar{P}_{Y|X}(A^c) P_X(\mathrm{d}x) \right] \end{aligned} \quad (12)$$

$$\begin{aligned} &= 1 + \inf_{P_X \in \mathcal{P}_X} \left[- \int_{\mathcal{X}} \bar{P}_{Y|X}(A^c) P_X(\mathrm{d}x) \right] \\ &= 1 - \sup_{P_X \in \mathcal{P}_X} \int_{\mathcal{X}} \bar{P}_{Y|X}(A^c) P_X(\mathrm{d}x) \\ &= 1 - \bar{\mathbb{E}}_X [\bar{P}_{Y|X}(A^c)], \end{aligned} \quad (13)$$

where (11) comes from the conjugacy property of lower probabilities, $\underline{P}(A) = 1 - \bar{P}(A^c)$, (12) comes from the additivity property of an integral, and (13) is true because for a generic function f , we have that $\sup -f = -\inf f$. In turn, this chain of equalities implies that

$$\mathbb{E}_X [P_{Y|X}(A)] = 1 - \bar{\mathbb{E}}_X [\bar{P}_{Y|X}(A^c)]. \quad (14)$$

Then, the following holds

$$\mathbb{E}_X [P_{Y|X}(A)] = 1 - \bar{\mathbb{E}}_X [\bar{P}_{Y|X}(A^c)] \quad (15)$$

$$\begin{aligned} &= 1 - \sup_{P_X \in \mathcal{P}_X} \int_{\mathcal{X}} \sup_{P_{Y|X} \in \mathcal{P}_{Y|X}} [P_{Y|X}(y \leq \underline{\Phi}(x) - \lambda\beta) + P_{Y|X}(y \geq \bar{\Phi}(x) + \lambda\beta)] P_X(\mathrm{d}x) \\ &\geq 1 - \sup_{P_X \in \mathcal{P}_X} \int_{\mathcal{X}} \bar{P}_{Y|X}(y \leq \underline{\Phi}(x) - \lambda\beta) P_X(\mathrm{d}x) - \sup_{P_X \in \mathcal{P}_X} \int_{\mathcal{X}} \bar{P}_{Y|X}(y \geq \bar{\Phi}(x) + \lambda\beta) P_X(\mathrm{d}x) \end{aligned} \quad (16)$$

$$\geq 1 - \frac{1}{\lambda\beta} \left[\sup_{P_X \in \mathcal{P}_X} \int_{\mathcal{X}} \bar{\mathbb{E}}_{Y|X}(\bar{m}) P_X(\mathrm{d}x) + \sup_{P_X \in \mathcal{P}_X} \int_{\mathcal{X}} \bar{\mathbb{E}}_{Y|X}(\underline{m}) P_X(\mathrm{d}x) \right] \quad (17)$$

$$= 1 - \frac{1}{\lambda\beta} \left[\frac{\beta}{2} + \frac{\beta}{2} \right] \quad (18)$$

$$= 1 - \frac{1}{\lambda}.$$

Equality (15) comes from (14). Inequality (16) comes from well-known properties of the sup operator. Inequality (17) comes from (9) and (10). Finally, equality (18) comes from (7) and (8). \square

Proof of Corollary 4. By Theorem 3 we have that $\mathbb{E}_X [P_{Y|X}(A)] \geq 1 - 1/\lambda$. In addition, by the properties of regular probabilities and upper probabilities, we have that $\bar{\mathbb{E}}_X [\bar{P}_{Y|X}(A)] \leq 1$. This implies immediately that $\bar{\mathbb{E}}_X [\bar{P}_{Y|X}(A)] - \mathbb{E}_X [P_{Y|X}(A)] \leq 1/\lambda$. \square

Proof of Corollary 5. We have that

$$\begin{aligned} \frac{1}{\lambda} &\geq \bar{\mathbb{E}}_X [\bar{P}_{Y|X}(y < \underline{\Phi}(x) - \lambda\beta, y > \bar{\Phi}(x) + \lambda\beta)] \\ &= \sup_{P_X \in \mathcal{P}_X} \int_{\mathcal{X}} \sup_{P_{Y|X} \in \mathcal{P}_{Y|X}} P_{Y|X}(y < \underline{\Phi}(x) - \lambda\beta, y > \bar{\Phi}(x) + \lambda\beta) P_X(\mathrm{d}x), \end{aligned} \quad (19)$$

where inequality (19) comes from Theorem 3. Now, by our assumption that both $\mathcal{P}_{\mathcal{X}}$ and $\mathcal{P}_{\mathcal{Y}|\mathcal{X}}$ are compact, there exist $\tilde{P}_X \in \mathcal{P}_{\mathcal{X}}$ and $P_{Y|X}^* \in \mathcal{P}_{\mathcal{Y}|\mathcal{X}}$ such that

$$\begin{aligned} & \sup_{P_X \in \mathcal{P}_{\mathcal{X}}} \int_{\mathcal{X}} \sup_{P_{Y|X} \in \mathcal{P}_{\mathcal{Y}|\mathcal{X}}} P_{Y|X}(y < \underline{\Phi}(x) - \lambda\beta, y > \overline{\Phi}(x) + \lambda\beta) P_X(dx) \\ &= \int_{\mathcal{X}} P_{Y|X}^*(y < \underline{\Phi}(x) - \lambda\beta, y > \overline{\Phi}(x) + \lambda\beta) \tilde{P}_X(dx). \end{aligned}$$

In addition, it follows immediately that

$$\begin{aligned} & \int_{\mathcal{X}} P_{Y|X}^*(y < \underline{\Phi}(x) - \lambda\beta, y > \overline{\Phi}(x) + \lambda\beta) \tilde{P}_X(dx) \\ & \geq \int_{\mathcal{X}} \alpha \mathbf{1} \left\{ P_{Y|X}^*(y < \underline{\Phi}(x) - \lambda\beta, y > \overline{\Phi}(x) + \lambda\beta) > \alpha \right\} \tilde{P}_X(dx) \\ &= \sup_{P_X \in \mathcal{P}_{\mathcal{X}}} \int_{\mathcal{X}} \alpha \mathbf{1} \left\{ \sup_{P_{Y|X} \in \mathcal{P}_{\mathcal{Y}|\mathcal{X}}} P_{Y|X}(y < \underline{\Phi}(x) - \lambda\beta, y > \overline{\Phi}(x) + \lambda\beta) > \alpha \right\} \tilde{P}_X(dx) \\ &= \overline{E}_X [\alpha \mathbf{1} \{ \overline{P}_{Y|X}(y < \underline{\Phi}(x) - \lambda\beta, y > \overline{\Phi}(x) + \lambda\beta) > \alpha \}]. \end{aligned}$$

By (19), this implies in turn that

$$\frac{1}{\lambda} \geq \overline{E}_X [\alpha \mathbf{1} \{ \overline{P}_{Y|X}(y < \underline{\Phi}(x) - \lambda\beta, y > \overline{\Phi}(x) + \lambda\beta) > \alpha \}],$$

which holds if and only if

$$\frac{1}{\lambda\alpha} \geq \overline{E}_X [\mathbf{1} \{ \overline{P}_{Y|X}(y < \underline{\Phi}(x) - \lambda\beta, y > \overline{\Phi}(x) + \lambda\beta) > \alpha \}],$$

concluding the proof. \square

B Additional Experimental Results

Implementation Details The control policies were trained using the Deep Deterministic Policy Gradient algorithm of 10^7 time steps, with a learning rate of 3×10^{-4} , and a buffer size of 10^7 . We used a 2-layer feedforward neural network with ReLU activation layers and a width of 256. The uncertainty maximization step in Algorithm 1 was performed with a timeout of 5×10^3 seconds, on a 96-core Intel Xeon Processor running at 3 GHz, and 800 GB RAM.

Additional Experimental Results We present additional results here. Table 4 and Table 5 summarize the coverage results of INN and CP in the in-distribution case. Additionally, Table 6, and Table 7 summarize the results when samples are drawn from a uniform distribution. This latter case, as we reiterate, is an out-of-distribution setting for CP, but is a within family distribution for INNs. As we observe that in some cases while CP fails provide coverage under 95%, INNs are observed to have much better coverage. However, this comes at the cost of slightly higher interval widths.

Environment	\mathcal{X} Dim	Conformal Prediction		INN (ours)	
		Coverage (%)	Interval Size	Coverage (%)	Interval Size
Ant	29	97	4.1	99	4.4
Half-Cheetah	18	94	4.9×10^{-1}	100	3.3
Hopper	12	95	1.6	100	2.5
Humanoid	47	93	1.8	99	3.1
Humanoid-Standup	47	97	158	99	248
Inverted Double Pendulum	6	95	6.8×10^{-3}	100	4.1×10^{-1}
Inverted Pendulum	4	95	1.3×10^{-4}	100	4.5×10^{-1}
Reacher	8	96	4.8×10^{-2}	100	4.3×10^{-1}
Swimmer	10	95	4×10^{-3}	100	4.1×10^{-1}
Walker2d	18	95	6	99	6.1

Table 4: We compare the coverage rates and size of prediction regions between an INN and CP for $\beta = 10^{-2}$ when the test samples are in-distribution. \mathcal{X} denotes the input space. The interval size of the INN is an average value across the samples.

Environment	\mathcal{X} Dim	Conformal Prediction		INN (ours)	
		Coverage (%)	Interval Size	Coverage (%)	Interval Size
Ant	29	95	3.9	99	4.3
Half-Cheetah	18	96	5.1×10^{-1}	99	4
Hopper	12	95	2.5	99	2.4
Humanoid	47	95	2.34	99.5	2.89
Humanoid-Standup	47	94	138	99	258
Inverted Double Pendulum	6	96	7×10^{-3}	100	3.55
Inverted Pendulum	4	97	2×10^{-4}	100	6.2×10^{-1}
Reacher	8	95	4.3×10^{-2}	100	4.8×10^{-2}
Swimmer	10	94	2.9×10^{-3}	100	9×10^{-2}
Walker2d	18	96	5.55	99	5.34

Table 5: We compare the coverage rates and size of prediction regions between an INN and CP for $\beta = 10^{-4}$ when the test samples are in-distribution. \mathcal{X} denotes the input space. The interval size of the INN is an average value across the samples.

Environment	\mathcal{X} Dim	Conformal Prediction		INN (ours)	
		Coverage (%)	Interval Size	Coverage (%)	Interval Size
Ant	29	97	4.1	100	4.6
Half-Cheetah	18	95	5.0×10^{-1}	100	1.56
Hopper	12	90	1.6	100	2.8
Humanoid	47	92	1.8	100	3.3
Humanoid-Standup	47	96	158	99	240
Inverted Double Pendulum	6	95	6.8×10^{-3}	100	4.1×10^{-1}
Inverted Pendulum	4	99	1.3×10^{-4}	100	4.5×10^{-1}
Reacher	8	98	4.9×10^{-2}	100	4.4×10^{-1}
Swimmer	10	96	4.4×10^{-3}	100	4.1×10^{-1}
Walker2d	18	99	6	98	5.2

Table 6: We compare the coverage rates and size of prediction regions between an INN and CP for $\beta = 10^{-2}$ when the test samples are out-of-distribution. \mathcal{X} denotes the input space. The interval size of the INN is an average value across the samples.

Environment	\mathcal{X} Dim	Conformal Prediction		INN (ours)	
		Coverage (%)	Interval Size	Coverage (%)	Interval Size
Ant	29	97	3.9	100	4.3
Half-Cheetah	18	96	5.2×10^{-1}	100	4.5
Hopper	12	95	2.5	100	2.5
Humanoid	47	96	2.3	100	2.93
Humanoid-Standup	47	95	137	100	263
Inverted Double Pendulum	6	96	7.1×10^{-3}	100	3.6
Inverted Pendulum	4	98	2.3×10^{-4}	100	6.2×10^{-1}
Reacher	8	98	4.9×10^{-2}	100	4.4×10^{-1}
Swimmer	10	96	4.4×10^{-3}	100	4.1×10^{-1}
Walker2d	18	94	5.5	100	5.5

Table 7: We compare the coverage rates and size of prediction regions between an INN and CP for $\beta = 10^{-4}$ when the test samples are out-of-distribution. \mathcal{X} denotes the input space. The interval size of the INN is an average value across the samples.